

# Searching for chemical relics of first stars with LAMOST and Subaru

Haining Li<sup>1,2</sup>, Wako Aoki<sup>3,4</sup>, Gang Zhao<sup>1</sup>, Satoshi Honda<sup>5</sup>, Norbert  
Christlieb<sup>6</sup> and Takuma Suda<sup>7</sup>

<sup>1</sup>Key Lab of Optical Astronomy, National Astronomical Observatories, Chinese Academy of  
Sciences, Beijing 100012, China

<sup>2</sup>email: [1hn@nao.cas.cn](mailto:1hn@nao.cas.cn)

<sup>3</sup>National Astronomical Observatory of Japan, 2-21-1 Osawa, Mitaka, Tokyo, 181-8588, Japan

<sup>4</sup>School of Physical Sciences, The Graduate University of Advanced Studies (SOKENDAI),  
2-21-1 Osawa, Mitaka, Tokyo 181-8588, Japan

<sup>5</sup>University of Hyogo, 407-2, Nishigaichi, Sayo-cho, Sayo, Hyogo, 679-5313, Japan

<sup>6</sup>Zentrum für Astronomie der Universität Heidelberg, Landessternwarte, Königstuhl 12,  
D-69117 Heidelberg, Germany

<sup>7</sup>Research Center for the Early Universe, The University of Tokyo, Hongo 7-3-1, Bunkyo-ku,  
Tokyo 113-0033, Japan

**Abstract.** We report progresses of a joint project on searching for extremely metal-poor (EMP) stars based on LAMOST survey and Subaru follow-up observation. Follow-up high-resolution snapshot spectra have been obtained for 70 objects, resulting in 42 EMP stars. A number of chemically interesting objects have already been identified, including (1) Two UMP (ultra metal-poor) stars with  $[\text{Fe}/\text{H}] \sim -4.0$ . One of them is the second UMP turnoff star with Li detection. (2) A super Li-rich ( $A(\text{Li}) \sim 3.1$ ) EMP giant. This is the most metal-poor and extreme example of Li enhancement in giants known to date, and will shed light on Li production during the evolution of red giants. (3) A few EMP stars showing extreme overabundance in heavy elements. Detailed abundances of these extreme objects and statistics obtained by the large sample of EMP stars will provide important constraints on the Galactic halo formation.

**Keywords.** stars:abundances, stars: Population II, nucleosynthesis

---

## 1. Introduction

Extremely metal-poor ( $[\text{Fe}/\text{H}]_{\dagger} < -3.0$ , EMP) stars are believed to record chemical and dynamical features of the early universe, since their atmosphere preserves signature of the gas at the time and place that they were born. EMP stars and stars with even lower metallicities such as ultra metal-poor ( $[\text{Fe}/\text{H}] < -4.0$ , UMP) and hyper metal-poor ( $[\text{Fe}/\text{H}] < -5.0$ , HMP) stars provide fundamental knowledge to the formation of first generation of stars (Frebel & Norris 2015), the nucleosynthesis yields of first supernovae (Nomoto *et al.* 2013), and the primordial nucleosynthesis model (Boesgaard & Steigman 1985).

It is now clear that a large fraction of stars with low metallicities present significant enhancements of carbon and are usually referred to carbon-enhanced metal-poor (CEMP) stars. There are also several subclasses of CEMP stars based on different abundance patterns of heavier elements, especially the neutron-capture elements (e.g., defined by Beers & Christlieb 2005), including CEMP-s (enriched in *s*-process elements), CEMP-

$\dagger [A/B] = \log(N_A/N_B)_{\star} - \log(N_A/N_B)_{\odot}$ , where  $N_A$  and  $N_B$  are the number densities of elements A and B respectively, and  $\star$  and  $\odot$  refer to the star and the Sun respectively

rs (enriched in both  $s$ - and  $r$ -process elements), and CEMP-no (no enhancement in neutron-capture elements). Statistical studies on CEMP stars have revealed that at lower metallicities, CEMP-no becomes dominant (Norris *et al.* 2013; Carollo *et al.* 2014). However, the origin of this subclass is not yet well understood (Masseron *et al.* 2010), although various models try to explain the observed abundance pattern, such as mass transfer from the AGB companion (Suda *et al.* 2004), carbon-rich winds of massive rotating EMP stars (Cescutti *et al.* 2013), and faint supernovae associated with first stars (Umeda & Nomoto 2005; Nomoto *et al.* 2013).

Abundances of the slow ( $s$ -) and rapid ( $r$ -) neutron-capture elements among metal-poor stars are very important to constrain early nucleosynthesis. Previous studies reveal that in the early Galaxy, the  $r$ -process is the primary contributor to the production of elements heavier than the iron group (Snedden *et al.* 1996). Only at higher metallicities (i.e., later time), the effect of  $s$ -process starts to emerge (Burris *et al.* 2000). A few stars have been found to exhibit extreme enhancements in  $r$ -process elements, e.g., the first  $r$ -process enhanced EMP giant found by Sneden *et al.* 1994, CS 22892–052 with a  $[\text{Eu}/\text{Fe}] \sim +1.6$ . Stars with  $[\text{Eu}/\text{Fe}] > +1$  and  $[\text{Ba}/\text{Eu}] < 0$  are referred to  $r$ -II stars (Beers & Christlieb 2005). An important result is that, the abundance pattern from Ba through Dy of the  $r$ -II stars is similar to the scaled solar system  $r$ -process (SSr) pattern. The astrophysical site of the  $r$ -process is not yet clear, but it is linked to explosive conditions of neutron star mergers (Goriely *et al.* 2013), or massive-star core-collapse supernovae (Woosley *et al.* 1994). Therefore,  $r$ -II stars are regarded as the best candidates to explore the nature of the  $r$ -process and its site.

Lithium abundances of metal-poor main-sequence turnoff stars provide important observational constraints on a number of basic questions, including the origin of different CEMP subclasses (e.g., Masseron *et al.* 2012; Hansen *et al.* 2014), the primordial Li production in the Big Bang nucleosynthesis (Asplund *et al.* 2006; Spite *et al.* 2013), etc. A plateau of lithium abundances around  $A(\text{Li}) \sim 2.2$  † has been observed among metal-poor main-sequence turnoff stars, and it seems to “meltdown” when it goes down to  $[\text{Fe}/\text{H}] < -3.0$  (Sbordone *et al.* 2010). On the other hand, red giants are expected to show low lithium abundances due to the first dredge-up which mixes the surface with internal Li-depleted material. However, a few metal-poor giants are found to show significant excess of lithium, which has raised challenges to the standard stellar evolution theory. Various modifications have been adopted to the standard model to explain the observed features of Li-rich giants at different evolutionary stages, including Charbonnel & Balachandran (2000) for the RGB bump, Nollett *et al.* (2003) for the AGB, Sackmann & Boothroyd (1999) for the RGB as well as extra mixing, etc.

## 2. Opportunity with LAMOST

Large scale survey including Hamburg/ESO survey (HES, Christlieb *et al.* 2008), and Sloan Digital Sky Survey and Sloan Extension for Galactic Understanding and Exploration (SDSS/SEGUE, Yanny *et al.* 2009) has tremendously increased the number of candidate metal-poor stars. High-resolution spectroscopic follow-up observations of these candidates have resulted in detailed chemical abundances of more than 300 EMP stars (e.g., Cayrel *et al.* 2004; Norris *et al.* 2013; Aoki *et al.* 2013; Roederer *et al.* 2014). However, EMP stars and metal-poor stars with peculiar chemical abundances are quite rare, e.g., the number of stars with  $[\text{Fe}/\text{H}] < -4.0$  is no larger than 20, and the number of identified metal-poor  $r$ -II stars is only 12. Hence additional EMP stars with extremely

†  $A(\text{Li}) = 12 + \log[n(\text{Li})/n(\text{H})]$  where  $n$  is the number density of atoms

low metallicities or peculiar abundance patterns are very important to further explore stellar evolution and the enrichment of the earliest Milky Way.

The Large sky Area Multi-Object fiber Spectroscopic Telescope, LAMOST † (also known as Wang-Su Reflecting Schmidt Telescope or Guoshoujing Telescope, Cui *et al.* 2012) started its 5-year regular survey in 2012 (Zhao *et al.* 2012). The unique design of LAMOST combines a 4-meter large aperture, a 5-degree field of view, and 4000 fibers on the focal plane. It can averagely observe about 3400 targets at one exposure, and thus allows to carry out large scale spectroscopic surveys of the Milky Way. Based on LAMOST low-resolution ( $R=1800$ ) spectra covering 3700–9100 Å, one can reliably identify candidate metal-poor stars in the survey mode, and hence notably enhance the searching efficiency. LAMOST has already obtained more than 3 million stellar spectra in the first two years, which is a huge database compared to previous stellar spectroscopic survey. More importantly, LAMOST survey is designed in such a way that the selection bias on spectral types (i.e., colors) are negligible (Carlin *et al.* 2012). Therefore it provides a great opportunity to enlarge the sample size of metal-poor stars and is also suitable for statistical studies.

We have selected more than 200 candidate metal-poor stars from the second data release of LAMOST spectroscopic survey. EMP candidates have been selected based on stellar parameters including metallicities determined from LAMOST spectra for all stars with S/N higher than 20 in the g-band, adopting methods by Li *et al.* (2015a).

### 3. Follow-up with Subaru and early results

For 70 of the selected candidate metal-poor stars, “snapshot” high-resolution spectra were acquired with the resolving power  $R=36,000$  and exposure times of 10–20 minutes during the two and half clear nights in May 2014 and March 2015 with the High Dispersion Spectrograph (HDS) at Subaru. This is similar to the observing mode as made by Aoki *et al.* (2013). After a quick visual check of the snap-shot spectra, a few interesting objects including two ultra metal-poor stars and a super Li-rich EMP star were selected out of the observed sample. Then for these targets, spectra with higher resolving power ( $R=60,000$ ) and higher signal-to-noise ratio covering 4000–6800 Å were further obtained for detailed abundance analysis.

Due to different signal-to-noise ratio and spectral quality of the snapshot spectra, stellar parameters have been estimated for 52 stars out of the 70 observed targets (with their location in  $T_{\text{eff}}$  vs.  $\log g$  diagram shown in Figure 1). The resultant metallicities confirm that all the measured 52 candidates are metal-poor, and there are 42 EMP stars with  $[\text{Fe}/\text{H}] < -3.0$ , including 17 with  $[\text{Fe}/\text{H}] < -3.5$  and 2 with  $[\text{Fe}/\text{H}] < -4.0$ . Such a result infers a very efficient selection, reaching a fraction of about 60% for the observed candidates and 80% for the targets whose parameters can be determined in identifying truly extremely metal-poor stars. It should be noted that the metallicity estimation depends on the determination of the effective temperature. The effective temperature is determined here using the spectroscopic method, i.e., by adjusting the temperature to make the Fe abundances derived from individual Fe I lines independent of the excitation potentials. For targets with fewer Fe I lines, more detailed analysis might result in different values of effective temperatures and metallicities.

The two UMP stars which were further observed with higher-resolution and higher-S/N include LAMOST J1253+0753, one new discovery to the other dozen of such rare objects, and LAMOST J1313–0552, an independent discovery of HE 1310–0520 (Hansen *et al.*

† See <http://www.lamost.org> for more detailed information, and the progress of the LAMOST surveys.

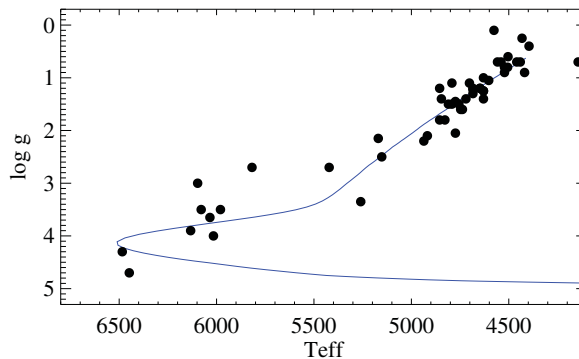


**Figure 1.** Distribution in the  $T_{\text{eff}}$  vs.  $\log g$  diagram of the 52 observed targets whose metallicities can be accurately determined from the Subaru snapshot spectra. A theoretical isochrone corresponding to a metallicity  $[\text{Fe}/\text{H}] \sim -3.0$  and an age of 13 Gyr (Demarque *et al.* 2004) is plotted for reference.

2014). Detailed abundance analysis shows that both UMP stars are carbon-enhanced, consistent with the scheme of higher fraction of CEMP stars at lower metallicities. The fact that neither of them shows an enhancement in neutron-capture elements support the result of previous studies that CEMP-no stars are dominant in the extremely low-metallicity region. Moreover, for the UMP turnoff LAMOST J1253+0753, we could determine its lithium abundance from the Li 6707 line ( $A(\text{Li}) \sim 1.80$ ) and thus make it the second UMP turnoff star with accurate Li abundance. As can be seen from the top left panel of Figure 2, this newly discovered UMP turnoff star is located below the observed Li plateau of metal-poor main-sequence turnoff stars, and provides unique evidence (the filled circle) to the so-called “meltdown” of the Li plateau around  $[\text{Fe}/\text{H}] \sim -4.2$  where there used to be no observational point before. The Li abundance of LAMOST J1253+0753 is very close to the value of another UMP main-sequence turnoff star HE 0233–0343 with  $A(\text{Li}) \sim 1.80$ . For the measured elements, both of the two UMP turnoff stars generally follow the “normal” pattern of metal-poor stars (Li *et al.* 2015b).

Another peculiar object which was selected from snapshot spectra and observed with  $R=60,000$  is LAMOST J0705+2552, a super Li-rich EMP star. This EMP giant shows extremely strong and saturated Li 6707 line with a large equivalent width of about 290 mÅ. Moreover, the Li 6103 line is also detectable in the spectra of this object. The lithium abundance of LAMOST J0705+2552 has thus been determined from the unsaturated Li 6103 line, resulting in  $A(\text{Li}) \sim 3.10$  (the filled star symbol in Figure 2). The lithium content of LAMOST J0705+2552 far exceeds the average lithium abundance of normal metal-poor giants (i.e.,  $A(\text{Li}) \sim 1.0$ , the dashed line in the top left panel) and the Li plateau of main-sequence turnoff stars ( $A(\text{Li}) \sim 2.2$ , the dash-dotted line), and makes it the most Li-rich giant with such low metallicity ( $[\text{Fe}/\text{H}] \sim -3.3$ ). Except for Li, LAMOST J0705+2552 also shows excess in abundances of N ( $[\text{N}/\text{Fe}] \sim 2.97$ ), Na ( $[\text{Na}/\text{Fe}] \sim 1.67$ ) and Mg ( $[\text{Mg}/\text{Fe}] \sim 0.96$ ). It is quite difficult to enhance nitrogen by the first dredge-up in EMP stars, and extra mixing would be necessary to enrich the surface of LAMOST J0705+2552 to reach such extreme enhancement in nitrogen (Suda & Fujimoto 2010). More interestingly, no nitrogen-enhanced metal-poor star has been reported to date showing large Li excess, and further detailed investigation on this object will help to understand the evolutionary status of this first super Li-rich nitrogen-enhanced EMP giant.

Among the observed 52 targets, we have also found an EMP star LAMOST J1109+0754 showing extreme enhancements in heavy elements. Although this object was only

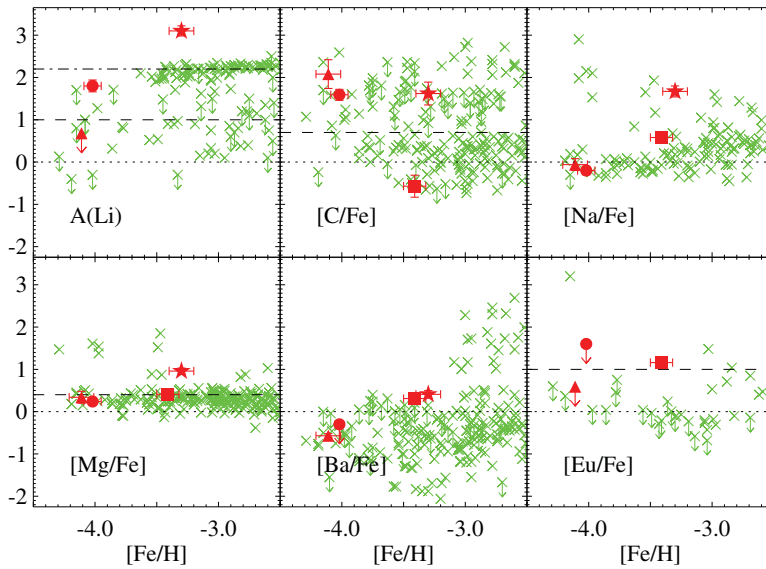


**Figure 2.**  $A(\text{Li})$  vs.  $[\text{Fe}/\text{H}]$  and  $[\text{X}/\text{Fe}]$  vs.  $[\text{Fe}/\text{H}]$  for C, Na, Mg, Ba and Eu. For lithium, the dashed line refers to the average  $A(\text{Li})$  among normal red giants with  $A(\text{Li}) \sim 1.0$ , and the dash-dotted line refers to the observed Li plateau around  $A(\text{Li}) \sim 2.2$ . For carbon, the dashed line refers to the division of carbon-enhanced and carbon-normal stars with  $[\text{C}/\text{Fe}] \sim +0.7$ . For Mg, the dashed line refers to the canonical value of  $[\alpha/\text{Fe}] \sim +0.4$  for the halo stars. Crosses correspond to literature metal-poor stars. Filled symbols correspond to the peculiar low-metallicity stars discovered and studied with LAMOST and Subaru, with the circle referring to LAMOST J1253+0753, the triangle referring to LAMOST J1313–0552, the square referring to LAMOST J1109+0754 and the star referring to LAMOST J0705+2552. Arrows correspond to upper or lower limits.

observed in snapshot mode, its being relatively bright enables us to obtain relatively high quality Subaru/HDS spectrum and to determine accurate parameters and elemental abundances for this object as well. Among the measured species, there are 11 elements in the nuclear charge range of  $Z = 38 - 66$ , covering the light trans-iron and the second  $r$ -process peak elements. The abundance pattern confirms that LAMOST J1109+0754 is a strongly  $r$ -process enhanced EMP star, e.g.,  $[\text{Eu}/\text{Fe}] = +1.16$  (filled square in Figure 2), and is very similar to that of literature cool  $r$ -II giants in the range from Sr through Dy (Li *et al.* 2015c). The abundance pattern of heavy elements of LAMOST J1109+0754 can also be well explained by the classical  $r$ -process. Therefore it is the thirteenth  $r$ -II star, with the lowest metallicity of  $[\text{Fe}/\text{H}] \sim -3.4$  among all  $r$ -II giants. The abundance pattern of LAMOST J1109+0754 from Ba through Dy well matches the theoretical SSr pattern, which provides additional evidence of a universal production ratio of these elements during the evolution of the Galaxy.

About 6 million stellar spectra will be obtained through LAMOST spectroscopic survey, and the joint collaboration with Subaru will certainly enable us to significantly enlarge the sample of EMP stars, and to explore the nature of the nucleosynthesis and chemical enrichment at the very beginning of the Universe.

## Acknowledgements

H.N.L. and G.Z. acknowledge supports by NSFC grants No. 11573032, 11233004, and 11390371. W.A. and T.S. are supported by the JSPS Grant-in-Aid for Scientific Research (S:23224004). S.H. is supported by the JSPS Grant-in-Aid for Scientific Research

(c:26400231). N.C. acknowledges support from Sonderforschungsbereich 881 “The Milky Way System” (subproject A4) of the German Research Foundation (DFG). Guoshoujing Telescope (the Large Sky Area Multi-Object Fiber Spectroscopic Telescope, LAMOST) is a National Major Scientific Project built by the Chinese Academy of Sciences. Funding for the project has been provided by the National Development and Reform Commission. LAMOST is operated and managed by the National Astronomical Observatories, Chinese Academy of Sciences. This work is based on data collected at the Subaru Telescope, which is operated by the National Astronomical Observatory of Japan.

## References

- Aoki, W., Beers, T. C., & Lee, Y. S., *et al.* 2013, *AJ*, 145, 13
- Asplund, Martin, Lambert, David L. & Nissen, Poul Erik, *et al.* 2006, *ApJ*, 664, 229
- Beers, T. C. & Christlieb, N. 2005, *ARA&A*, 43, 531
- Boesgaard, A. M. & Steigman, G. 1985, *ARA&A*, 23, 319
- Bromm, V. & Yoshida, N. 2011, *ARA&A*, 49, 373
- Burris, D. L., Pilachowski, C. A., & Armandroff, T. E., *et al.* 2000, *ApJ*, 544, 302
- Carlin, J. L., Lpine, S., & Newberg, H. J., *et al.* 2012, *RAA*, 12, 775
- Carollo, D., Freeman, K., & Beers, T. C., *et al.* 2014, *ApJ*, 788, 180
- Cayrel, R., Depagne, E., Spite, M., *et al.* 2004, *A&A*, 416, 1117
- Cescutti, G., Chiappini, C., & Hirschi, *et al.* 2013, *A&A*, 553, A51
- Charbonnel, C. & Balachandran, S. C. 2000, *A&A*, 359, 563
- Christlieb, N., Schreck, T., Frebel, A., *et al.* 2008, *A&A*, 484, 721
- Cui, X.-Q., Zhao, Y.-H., & Chu, Y.-Q., *et al.* 2012, *RAA*, 12, 1197
- Frebel, A. & Norris, J. E. 2015, *ARA&A*, in press, arXiv:1501.06921
- Goriely, S., Sida, J.-L., & Lematre, J.-F., *et al.* 2013, *Physical Review Letters*, 111, 242502
- Hansen, T., *et al.* 2014, *ApJ*, 787, 162
- Li, H. N., Zhao, G., Christlieb, N., *et al.* 2015a, *ApJ*, 798, 110
- Li, H. N., Aoki, W., Zhao, G., *et al.* 2015b, *PASJ*, in press, arXiv:1506.05684
- Li, H. N., Aoki, W., Honda, S., *et al.* 2015c, *RAA*, 15, 1264
- Masseron, T., Johnson, J. A., Plez, B., *et al.* 2010, *A&A*, 509, A93
- Masseron, T., Johnson, J. A., Lucatello, S., *et al.* 2012, *ApJ*, 751, 14
- Nollett, Kenneth M., Busso, M., & Wasserburg, G. J. 2003, *ApJ*, 582, 1036
- Nomoto, K., Kobayashi, C., & Tominaga, N. 2013, *ARA&A*, 51, 457
- Norris *et al.* 2013a, *ApJ*, 762, 28
- Norris *et al.* 2013b, *ApJ*, 762, 25
- Roederer, I. U., Cowan, J. J., & Preston, G. W., *et al.* 2014, *MNRAS*, 445, 2970
- Sackmann, I.-Juliana & Boothroyd, Arnold I. 1999, *ApJ*, 510, 217
- Sbordone, L., Bonifacio, P., Caffau, E., *et al.* 2010, *A&A*, 522, 26
- Snedden, C., Preston, G. W., McWilliam, A., & Searle, L. 1994, *ApJ*, 431, L27
- Snedden, C., McWilliam, A., & Preston, G. W., *et al.* 1996, *ApJ*, 467, 819
- Spite, M., Caffau, E., Bonifacio, P., *et al.* 2013, *A&A*, 552, A107
- Suda, T., Aikawa, M., & Machida, M. N., *et al.* 2004, *ApJ*, 611, 476
- Suda, T. & Fujimoto, M. Y. 2010, *MNRAS*, 405, 177
- Umeda, H. & Nomoto, K. 2005, *ApJ*, 619, 427
- Woosley, S. E., Wilson, J. R., & Mathews, G. J., *et al.* 1994, *ApJ*, 433, 229
- Yanny, B., Rockosi, C., & Newberg, H. J., *et al.* 2009, *ApJ*, 137, 4377
- Yong, D., *et al.* 2013, *ApJ*, 762, 27
- Zhao, G., Zhao, Y. H., & Chu, Y. Q., *et al.* 2012, *RAA*, 12, 723